
Figures and figure supplements

Defective mesenchymal Bmpr1a-mediated BMP signaling causes congenital pulmonary cysts

Yongfeng Luo et al.

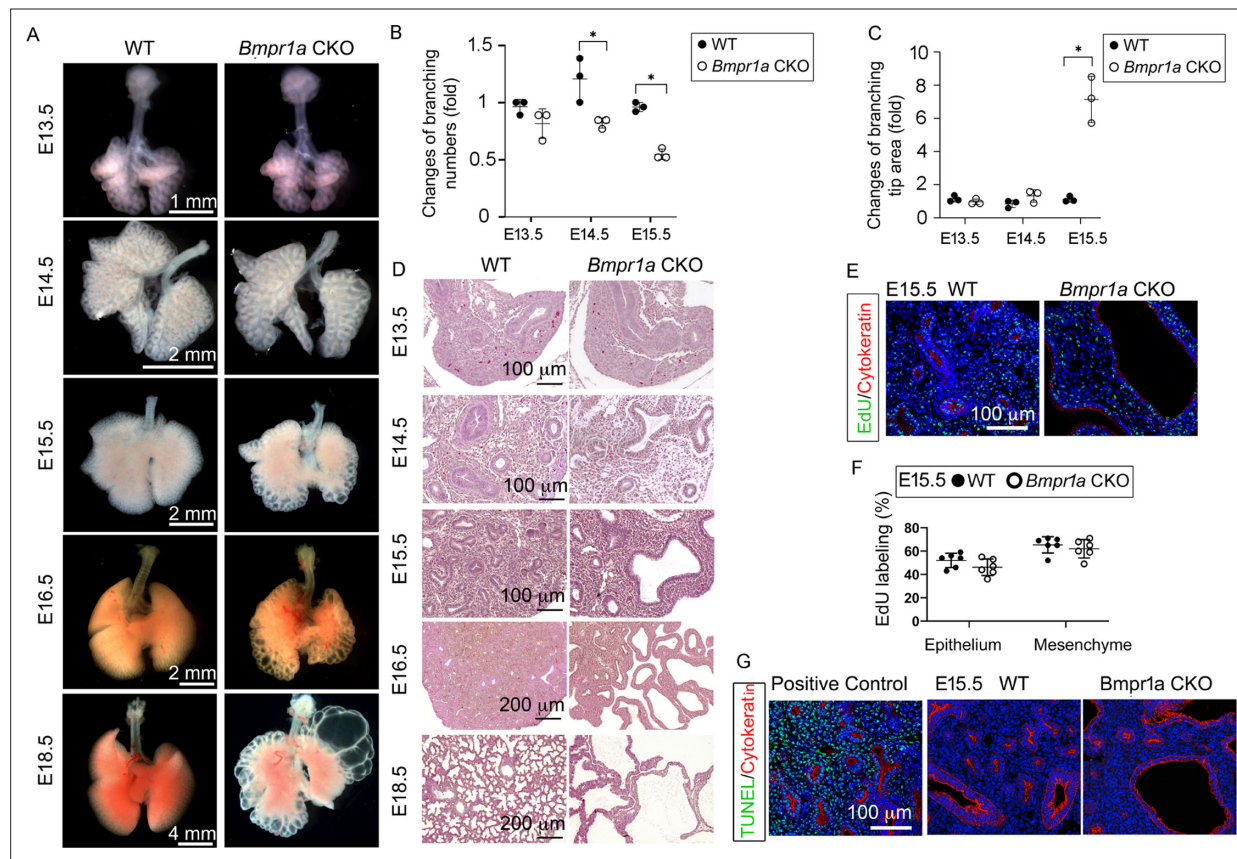


Figure 1. Lung mesenchyme-specific deletion of *Bmpr1a* caused abnormal lung morphogenesis and prenatal airway cystic lesions beginning in mid-gestation. **(A)** Brightfield images of whole wildtype (WT) and *Bmpr1a* conditional knockout (CKO) mouse lungs at different embryonic stages. **(B and C)** Quantitative measurement and comparison of terminal airway branching numbers and sizes. **(D)** Hematoxylin and eosin (H&E)-stained *Bmpr1a* CKO lungs at different embryonic stages. **(E and F)** EdU incorporation study for cell proliferation analysis in lung mesenchymal and cytokeratin-positive epithelial cells (n=6). **(G)** Apoptosis analysis by TUNEL assay. The positive control slides for apoptosis were generated by treating the tissue sections with DNase I. Pictures are representative of at least five samples in each condition.

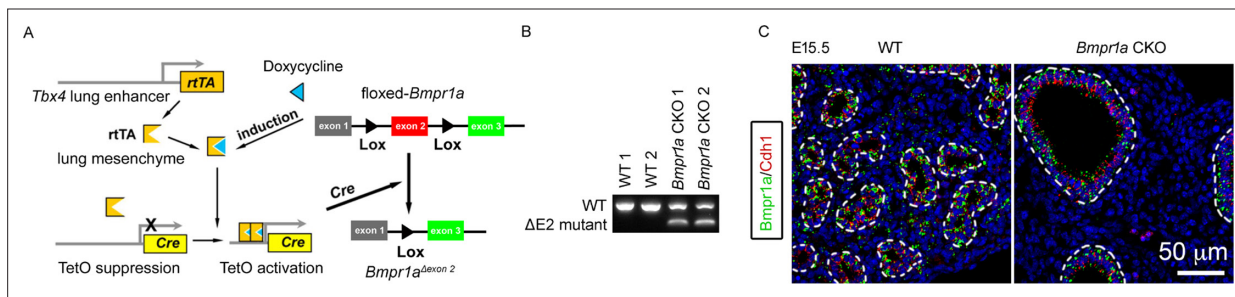


Figure 1—figure supplement 1. *Bmpr1a* was specifically deleted in lung mesenchymal cells. **(A)** Schematic representation of the lung mesenchyme-specific knockout of *Bmpr1a* by *Tbx4*-*rtTA*/*Teto*-*Cre* driver line. **(B)** Verification of *Bmpr1a* genetic deletion at the mRNA level. Δ E2: exon 2 deletion. **(C)** Immunostaining of *Bmpr1a* (green) and *Cdh1* (red). The airways are highlighted with dot lines.

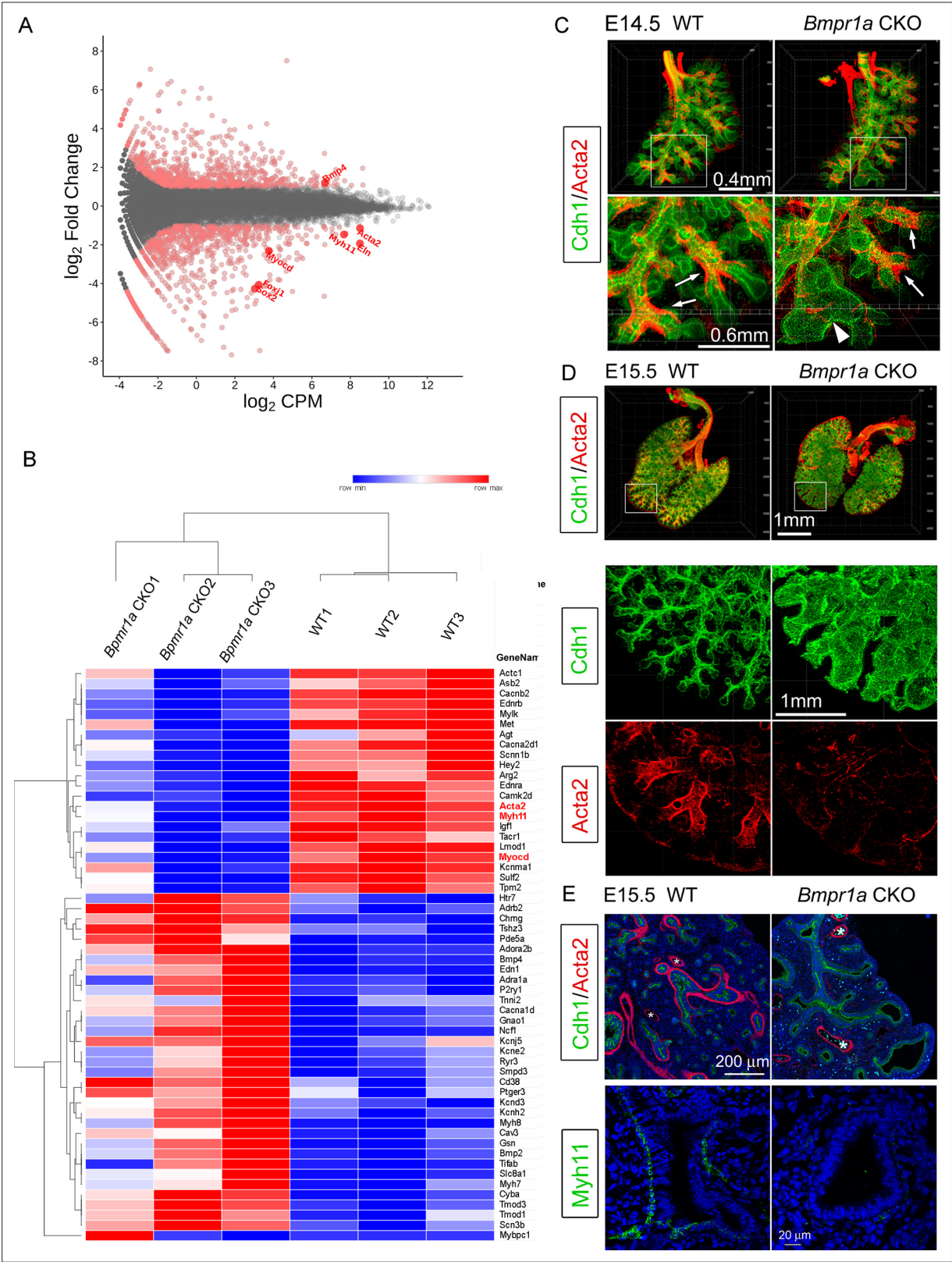


Figure 2. Airway smooth muscle was substantially reduced in *Bmpr1a* conditional knockout (CKO) lungs. **(A)** Scatter plots of RNA-seq analysis for differentially expressed genes (DEGs) (n=3). **(B)** RPKM heatmap of Muscle System Process Genes (GO:0003012). Genes involved in the Muscle System Process with significant changes between *Bmpr1a* CKO and wildtype (WT) lungs are shown in the RNA-seq heatmap. The input data was RPKM values generated from the raw data using the R/Bioconductor program ‘edgeR’. **(C and D)** Whole mount immunostaining of Cdh1 and Acta2 in embryonic day 14.5 (E14.5) WT and *Bmpr1a* CKO lungs. **(E)** Whole mount immunostaining of Cdh1 and Acta2 in embryonic day 15.5 (E15.5) WT and *Bmpr1a* CKO lungs. Figure 2 continued on next page

Figure 2 continued

(E)14.5 and E15.5 lungs. Excessive dilation of airway terminals and extensive reduction of airway smooth muscle were observed in E15.5 *Bmpr1a* CKO lungs. The normal-looking airways are marked by arrows and the enlarged epithelial bud accompanied with compromised smooth muscle are marked by arrowheads. (E) E15.5 lung section stained with Cdh1& Acta2 or Myh11. *Vascular structures.

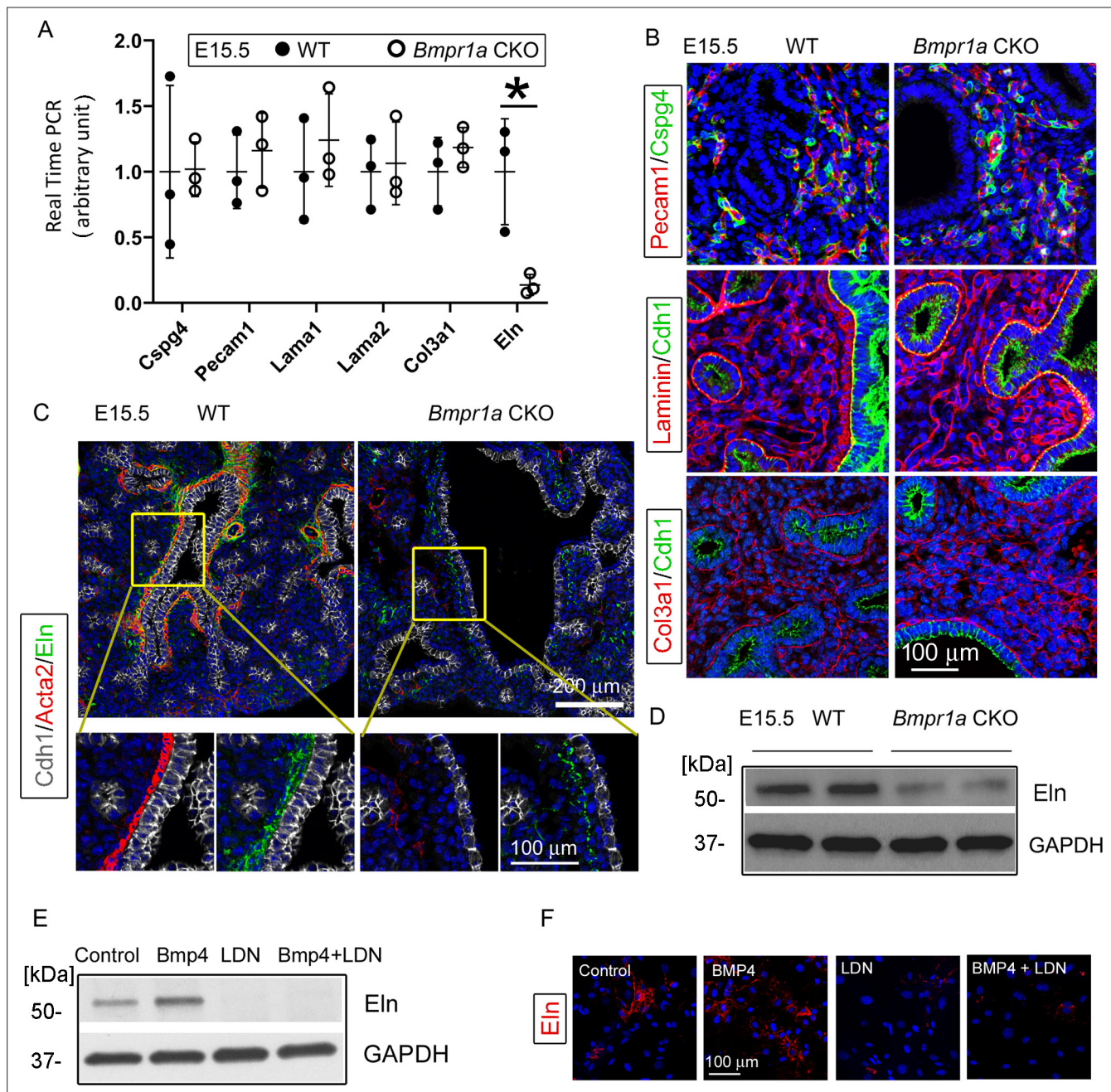


Figure 3. *Bmpr1a* conditional knockout (CKO) resulted in a significant reduction in elastin expression underneath the airway epithelia of embryonic day (E)15.5 lungs, but not in the pericytes, vasculature, and basement membrane. **(A)** Expression of *Cspg4*, *Pecam1*, *Lama1*, *Lama2*, *Col3a1*, and *Eln* at the mRNA level was measured by real-time PCR, *p<0.05. **(B)** E15.5 lung section stained with Cspg4, Pecam1, laminin, and Col3a1. **(C)** E15.5 lung section stained with Cdh1, Acta2, and elastin. **(D)** Reduced elastin expression of *Bmpr1a* CKO lungs at the protein level was detected by western blot (WB). **(E and F)** Elastin expression in E15.5 lung mesenchymal cells was upregulated by BMP4 and downregulated by BMP type 1 receptor-specific inhibitor LDN193189 (LDN), as detected by WB and immunofluorescence staining.

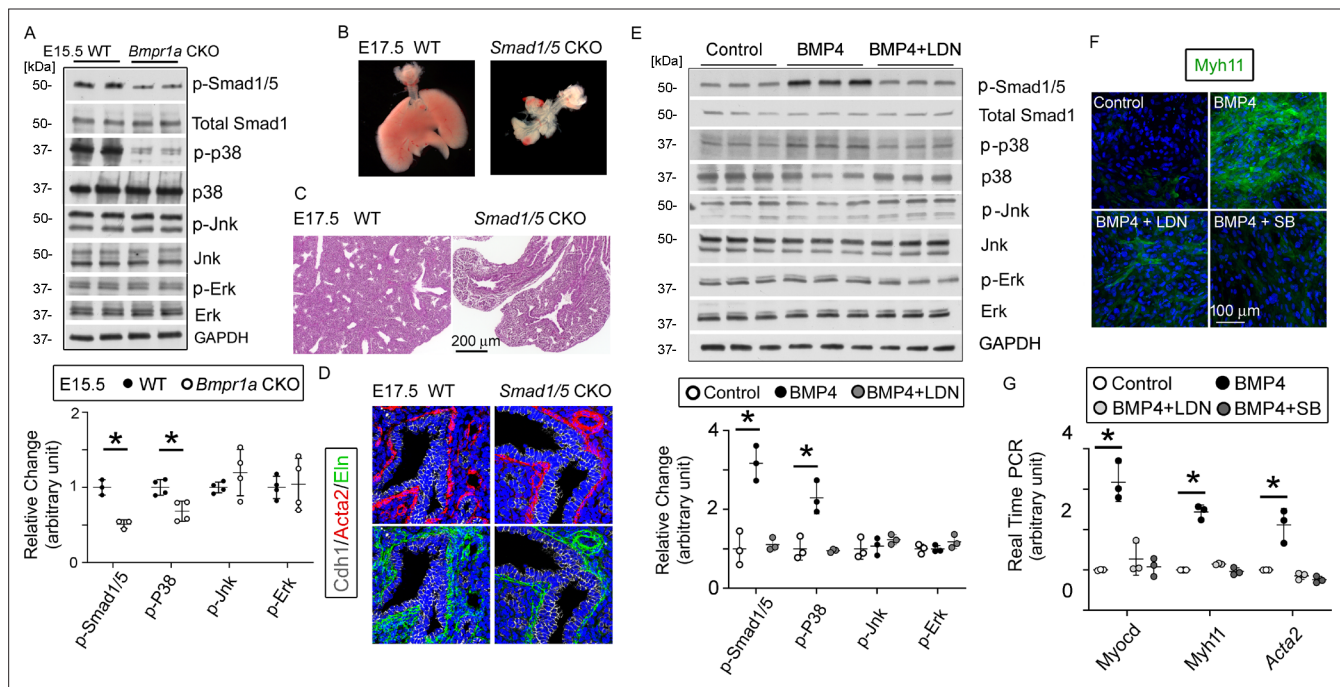


Figure 4. The bone morphogenetic protein (BMP) pathway regulates the myogenesis of lung mesenchymal cells via the Smad-independent pathway. **(A)** Activation of the intracellular downstream Smad1, p38, Jnk, and Erk signaling pathways in wildtype (WT) and *Bmpr1a* conditional knockout (CKO) lung tissues was detected by the western blot (WB) and quantified by densitometry. The levels of protein phosphorylation were normalized by the corresponding total protein and is presented as a relative change to the WT, * $p < 0.05$. **(B)** Gross view of whole lungs from *Smad1/5* double conditional knockout mice (*Smad1/5* CKO) and WT littermates showed that simultaneous deletion of *Smad1* and *Smad5* in lung mesenchyme completely disrupted lung development. **(C)** No airway dilation or cysts were observed in the hematoxylin and eosin (H&E)-stained tissue sections of the *Smad1/5* CKO lungs at embryonic day (E)17.5. **(D)** Expression of airway smooth muscle cells (SMCs) and elastin was not altered in E17.5 *Smad1/5* CKO lungs, as shown by immunostaining of Cdh1, Acta2, and elastin. **(E)** Changes of intracellular signaling pathways in cultured fetal lung mesenchymal cells upon treatment with BMP4 (50 ng/ml) and/or LDN193189 (200 nM) were detected by WB and quantified by densitometry. The relative change to the control condition is presented, * $p < 0.05$. **(F and G)** Altered expression of SMC genes at the protein level (Myh11) and the mRNA level (*Myocd*, *Myh11*, and *Acta2*) was respectively analyzed by immunostaining and real-time PCR for the primary culture of E15.5 WT lung mesenchymal cells treated with BMP4 (50 ng/ml), LDN (200 nM), and SB (1 μ M), * $p < 0.05$.

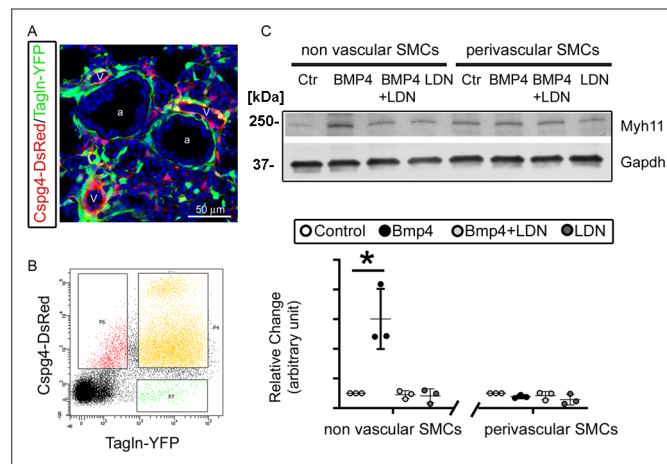


Figure 5. Bmpr1a-mediated signaling played different roles in the differentiation of airway versus vascular smooth muscle cells (SMCs). **(A)** YFP and DsRed expression patterns in the fetal lungs of *Tagln-YFP/Cspg4-DsRed* mice. a: airway, v: vessel. **(B)** Airway SMCs (YFP⁺) and vascular SMCs (YFP⁺/DsRed⁺) were isolated by fluorescence-activated cell sorting (FACS). **(C)** The differential effect of Bmp4 treatment (50 ng/ml) on contractile protein Myh11 expression was analyzed in SMCs of non-vascular origin (YFP⁺) versus vascular origin (YFP⁺/DsRed⁺), and the role of Bmpr1a in mediating this effect was tested by adding its specific inhibitor LDN193189 (200 nM). The western blot (WB) data of Myh11 expression was normalized to GAPDH (loading control) and is represented as a relative change to the control condition, *p<0.05.

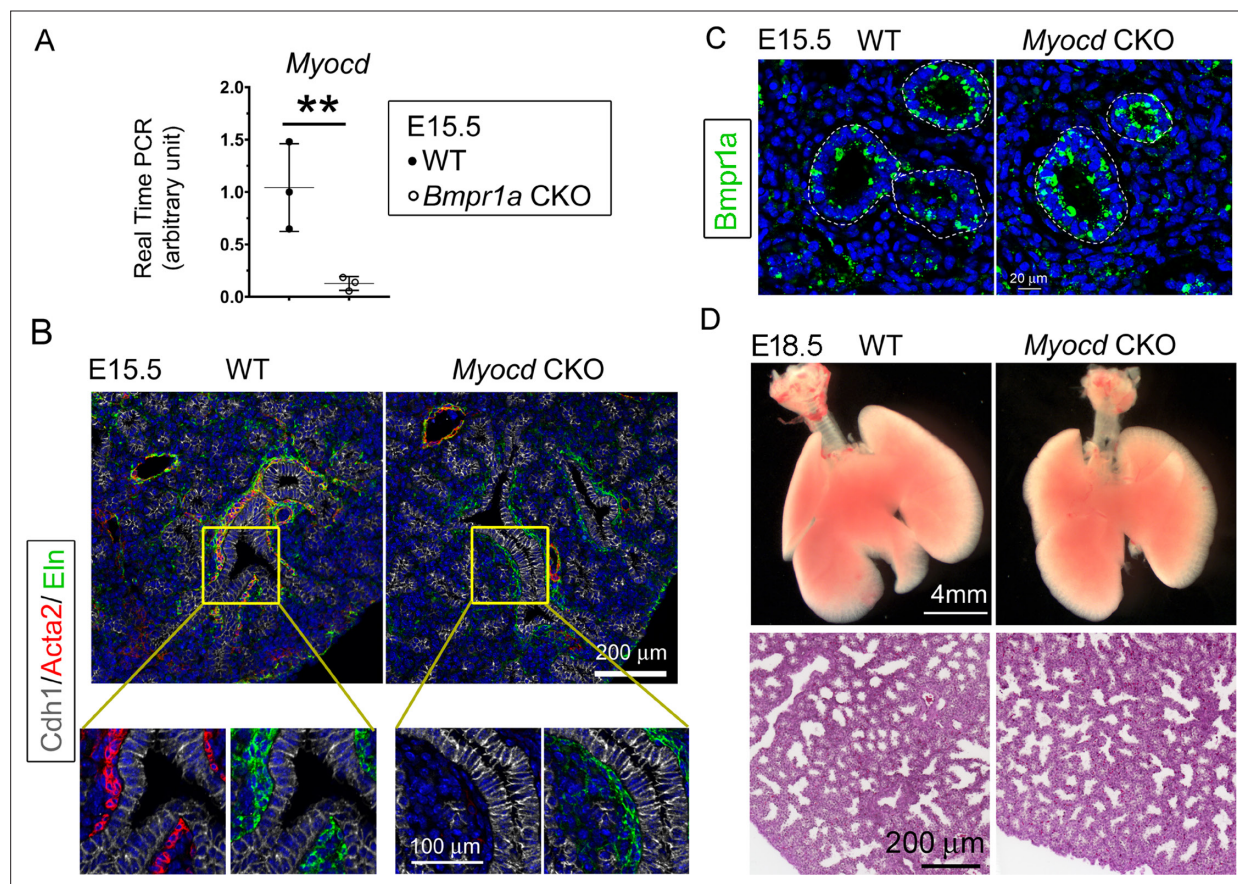


Figure 6. Lung mesenchymal knockout of *Myocd* did not cause any branching abnormalities or lung cysts. **(A)** The expression of *Myocd* in *Bmpr1a* conditional knockout (CKO) lungs was substantially decreased, as measured by real-time PCR, $**p < 0.01$. **(B)** Deficiency in airway smooth muscle cells (SMCs) was observed in embryonic day (E)15.5 mesenchyme-specific *Myocd* CKO lungs, as shown by co-immunofluorescence staining of Cdh1, Acta2, and elastin. **(C)** Comparison of *Bmpr1a* expression between E15.5 *Myocd* CKO and wildtype (WT) control lungs by immunofluorescence staining. **(D)** Comparison of the lungs between WT and *Myocd* CKO mice at the end of gestation (E18.5) did not reveal any significant morphological changes by gross view. No histological difference was found between the WT and the *Myocd* CKO lungs by examining their hematoxylin and eosin (H&E)-stained lung tissue sections.

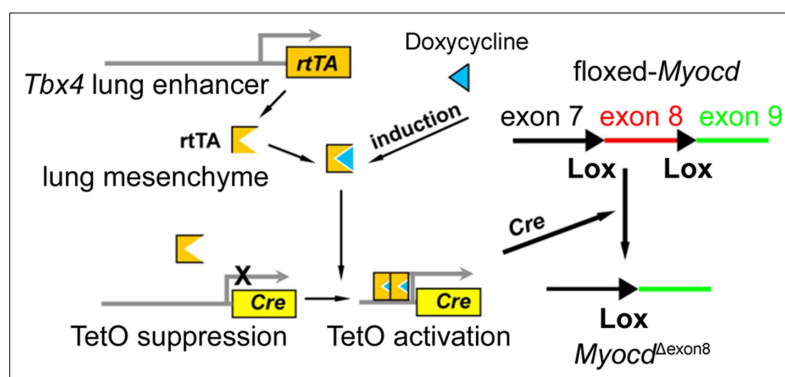


Figure 6—figure supplement 1. Schematic representation of the lung mesenchyme-specific knockout of *Myocd* by *Tbx4-rtTA/Teto-Cre* driver line.

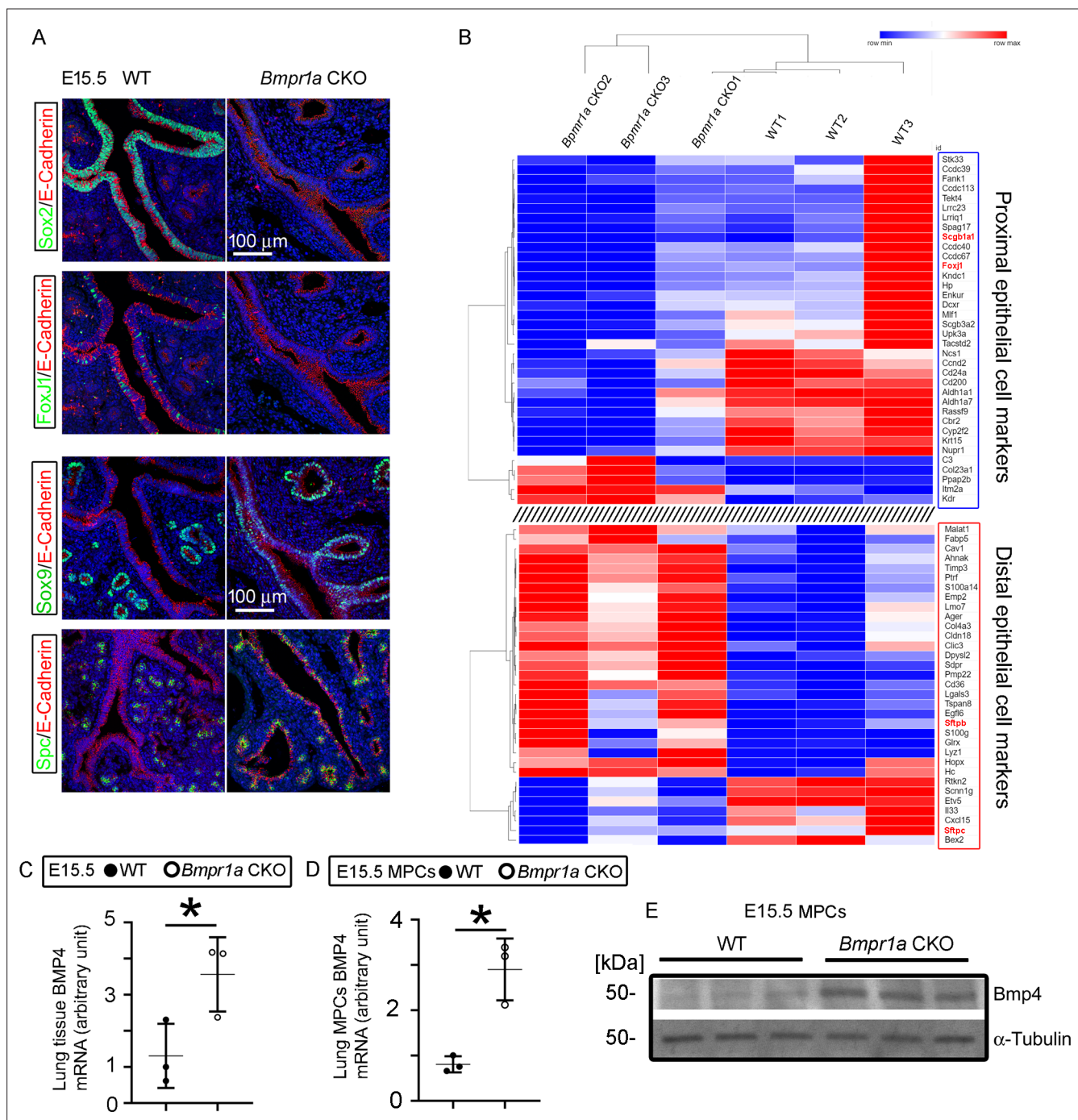


Figure 7. Mesenchymal *Bmpr1a* deletion disrupted airway epithelial proximal-distal differentiation and development. **(A)** Proximal epithelial cells, marked by Sox2 and Foxj1 staining, were significantly decreased in the proximal portion of the airways in embryonic day (E)15.5 *Bmpr1a* conditional knockout (CKO) lungs. Ectopic distribution of distal epithelial cells marked by Sox9 and Spc staining was detected in the proximal airways of E15.5 *Bmpr1a* CKO lungs. **(B)** Heatmap of RNA-seq data showing significant changes in the marker genes of proximal and distal epithelial cells. **(C)** Increased *Bmp4* expression at the mRNA level was detected in E15.5 *Bmpr1a* CKO lung tissue by RT-PCR. **(D and E)** *Bmp4* expression in isolated fetal lung mesenchymal cells with genotypes of wildtype (WT) vs. *Bmpr1a* CKO was analyzed at both the mRNA and protein levels by RT-PCR and western blot (WB) respectively.